CrystEngComm

Cite this: *CrystEngComm*, 2011, **13**, 3156

www.rsc.org/crystengcomm

PAPER

Selectivity of amides by host–guest inclusion†

Nikoletta B. Báthori* and Luigi R. Nassimbeni

Received 1st July 2010, Accepted 20th September 2010
DOI: 10.1039/c0ce00362j

The mechanism of selectivity by enclathration of four amides, *N*-methylformamide (NMF), dimethylformamide (DMF), *N*-methylacetamide (NMA) and dimethylacetamide (DMA), has been investigated by employing a bulky, flexible host. We measured the two-component selectivity curves for a mixture of amides, whose proportions in the crystals were determined by ^{1}H NMR spectroscopy. The crystal structures of the single guest inclusion compounds were elucidated and analyzed. The subtle changes in the torsional flexibility of the host were correlated to the selectivity. The packing factor, which represents the occupied *vs.* available space by the guest in the crystal structures correlates with the measured selectivities.

Introduction

Systematic studies of selectivity by enclathration commonly involve lattice energy calculations,[1] comparison of hydrogen bond networks and packing motifs of crystals.[2] Detailed study of weaker, non-bonding interactions (for example interactions between aromatic rings) is often neglected or poorly analyzed when a well defined hydrogen bond network can be recognized in the crystal structure. However, these interactions may make a significant contribution to the packing forces, and hence to physico-chemical properties of the system, such as selectivity.

The selectivity of a given guest from a mixture by a host compound has great interest in the field of crystal engineering[3] and may be studied by analyzing the non-bonded interactions that occur in solid host–guest compounds.[4] A convenient measure of this selectivity is given by the selectivity coefficient, $K_{A:B}$, and defined as:

$$K_{A:B} = (K_{B:A})^{-1} = Z_A/Z_B \times X_B/X_A$$

where for two guests A and B, X_A and X_B are the mole fractions in the mother liquor and Z_A and Z_B are the mole fractions of the guests entrapped in the crystal.[5]

When hydrogen-bonding occurs between host and guest, this is an important factor of the molecular recognition occurring between the main components of the inclusion compound. However, using a bulky host compound with flexible aromatic rings and well known hydrogen bond donor properties yields the opportunity to investigate the mechanism of inclusion complexation *via* molecular recognition. It is therefore of interest to compare the selectivities of a host possessing a hydroxyl H-bond donor moiety with a series of amides whose structures are closely related. We thus chose *N*-methylformamide (NMF), dimethylformamide (DMF), *N*-methylacetamide (NMA) and dimethylacetamide (DMA) as our guests and carried out a series of enclathration experiments with the host **H**, (*R*,*R*)-(−)-*trans*-2,3-bis(hydroxydiphenylmethyl)-1,4-dioxaspiro(4,5)decane. This compound has been employed in the resolution of various bicyclic enones.[6] The molecular schematics are shown in Scheme 1.

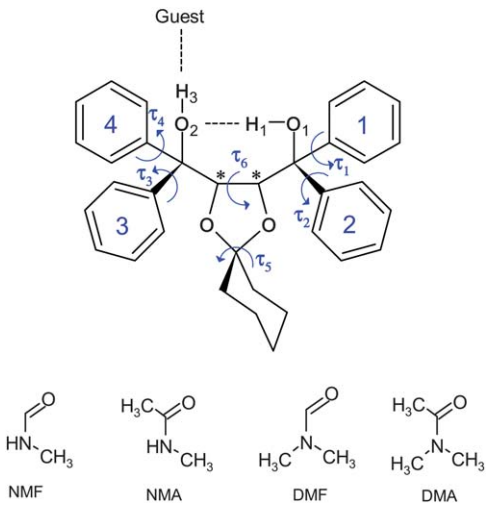

Scheme 1

Methods

In the competition experiments the relative proportions of solvent molecules were measured on a 400 MHz Varian NMR instrument by integrating the signal from the –NH, the –CHO or

Department of Chemistry, Faculty of Applied Sciences, Cape Peninsula University of Technology, P.O. Box 652, Cape Town, 8000, South Africa. E-mail: bathorin@cput.ac.za; Fax: +27 21 460 3854; Tel: +27 21 460 8354

† CCDC reference numbers 782737–782740. For crystallographic data in CIF or other electronic format see DOI: 10.1039/c0ce00362j

Table 1 Crystallographic data for solvates

	H·NMF	H·NMA	H·DMF	H·DMA
CCDC no.	782737	782738	782739	782740
Host : guest ratio	1 : 1	1 : 1	1 : 1	1 : 1
Chemical formula	$C_{36}H_{39}N_1O_5$	$C_{37}H_{41}N_1O_5$	$C_{37}H_{41}N_1O_5$	$C_{38}H_{43}N_1O_5$
Formula weight	565.68	579.71	579.71	593.73
Temperature/K	173(2)	173(2)	173(2)	173(2)
Crystal system	Monoclinic	Monoclinic	Orthorhombic	Triclinic
Space group (no.)	$P2_1$ (no. 4)	$P2_1$ (no. 4)	$P2_12_12_1$ (no. 19)	$P1$ (no. 1)
a/Å	9.3699(14)	9.3986(10)	9.6500(12)	9.4536(19)
b/Å	32.679(5)	33.587(4)	10.6523(12)	9.946(2)
c/Å	10.0882(15)	10.0932(10)	29.701(4)	17.296(4)
α/°	90.00	90.00	90.00	98.88(3)
β/°	93.835(4)	94.981(2)	90.00	98.57(3)
γ/°	90.00	90.00	90.00	91.31(3)
V/Å^3	3082.1(8)	3174.1(6)	3053.1(6)	1587.2(6)
Z'/Z	2/4	2/4	1/4	2/2
D_{calc}/Mg m^{-3}	1.219	1.213	1.261	1.242
Radiation type	MoKα	MoKα	MoKα	MoKα
$F(000)$	1208	1240	1240	636
Crystal size/mm	0.5 × 0.5 × 0.5	0.18 × 0.02 × 0.02	0.5 × 0.5 × 0.5	0.5 × 0.5 × 0.5
Colour, crystal form	Colourless, chunk	Colourless, plates	Colourless, chunk	Colourless, chunk
No. of total reflections	6369	6127	3541	5398
No. of unique reflections	5002	4461	3162	5211
$\Theta_{min-max}$/°	2.02/26.42	2.03/25.68	2.03/26.41	2.07/24.71
$R[F^2 > 2\sigma(F^2)]$, w$R(F^2)$, S	0.0398, 0.0785, 1.085	0.0469, 0.0924, 1.133	0.0320, 0.0729, 1.097	0.0266, 0.0659, 1.060
No. of parameters	799	796	425	914
Res. peak (max/min)/e Å^{-3}	0.170/−0.199	0.429/−0.315	0.034/−0.181	0.152/−0.144

the methyl protons of the guests. The proportion of the host compound was measured by integrating the protons bonded to the chiral carbon atoms at 4.6 ppm. X-Ray diffraction data for compounds were collected on a Bruker DUO APEX II diffractometer[7] with graphite-monochromated MoKα_1 radiation (λ = 0.71073 Å) at 173 K using an Oxford Cryostream 700. Data reduction and cell refinement were performed using SAINT-Plus.[8] The space groups were determined from systematic absences by XPREP[9] and further justified by the refinement results. The structures were solved using SHELXS-97[10] and refined using full-matrix least squares method in SHELXL-97[10] with the aid of the program X-Seed.[11] The hydrogen atoms bound to carbon atoms were placed at idealized positions and refined as riding atoms with $U_{iso}(H) = 1.2\ U_{eq}$(Ar–H, CH_2) or 1.5 $U_{eq}(CH_3)$. The refinement of the hydroxyl hydrogen atoms was carried out by first locating them on a difference electron density map and subsequently imposing an appropriate O–H bond length constraint. Diagrams and publication material were generated using PLATON[12] and X-Seed.

Structures

The crystal and refinement data are given in Table 1. The structure of H·NMF crystallises in the space group $P2_1$ with Z = 4. There are thus two independent host and guest molecules in

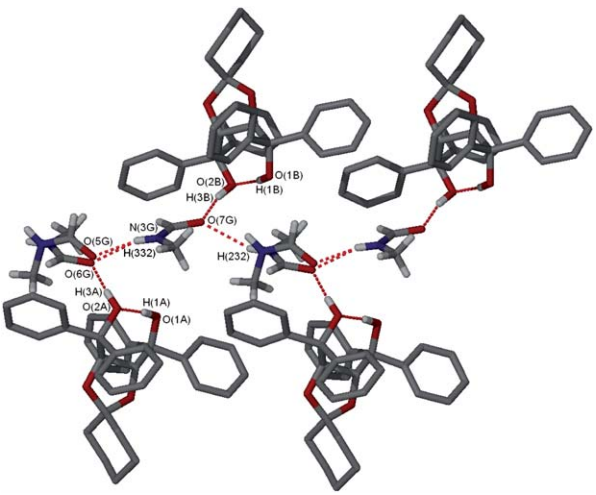

Fig. 1 $C_2^2(8)$ Hydrogen bond pattern in H·NMF.

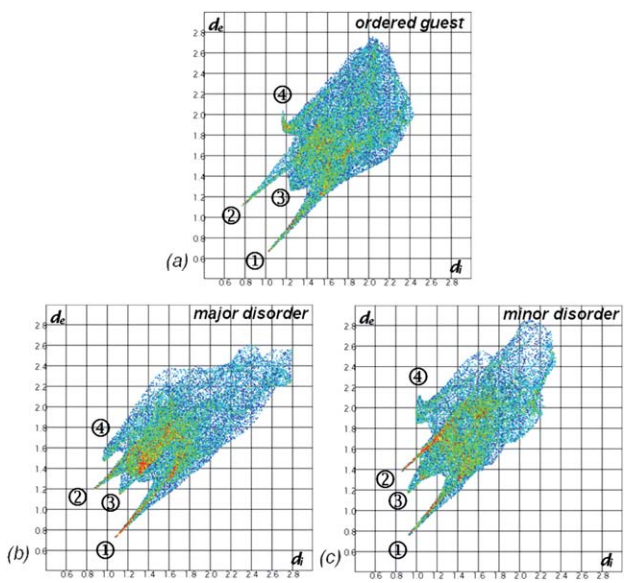

Fig. 2 Fingerprint plots of guest molecules of structure H·NMF.

Table 2 Hydrogen bond metrics

D–H···A H·NMF	D–H/Å	H···A/Å	D···A/Å	D–H···A/°	Description
O1A–H1A···O2A	0.92	1.77	2.687(2)	174.2	Intramolecular
O2A–H3A···O6G	0.86	1.80	2.622(16)	161.9	Host–guest
O1B–H1B···O2B	0.90	1.78	2.663(3)	166.5	Intramolecular
O2A–H3A···O5G	0.86	1.94	2.774(11)	164.2	Host–guest
N3G–H332···O5G	0.88	2.02	2.874(12)	163.9	Guest–guest
N3G–H332···O6G	0.88	2.18	3.016(16)	159.6	Guest–guest
O2B–H3B···O7G	0.89	1.79	2.662(3)	164.8	Host–guest
N1G–H132···O7G*[a]	0.88	2.19	2.966(4)	146.2	Guest–guest
N2G–H232···O7G*[a]	0.88	2.37	3.216(11)	160.7	Guest–guest
O1B–H1B···O2B	0.90	1.78	2.663(3)	166.5	Intramolecular
H·NMA					
O1A–H1A···O2A	0.85(4)	1.82(6)	2.659(4)	170(5)	Intramolecular
O2A–H3A···O5	0.92(5)	1.78(5)	2.637(4)	154(5)	Host–guest
N1–H132···O1B*[a]	0.88	2.16	3.011(5)	162.7	Host–guest
N2–H232···O1A	0.88	2.11	2.981(7)	172.1	Host–guest
O1B–H1B···O2B	0.87(6)	1.88(6)	2.666(4)	164(6)	Intramolecular
O2B–H3B···O6	0.90(6)	1.77(6)	2.646(4)	164(5)	Host–guest
H·DMF					
O1–H1···O2	0.84(3)	1.91(3)	2.731(2)	168(3)	Intramolecular
O2–H3···O5	0.86(3)	1.80(3)	2.652(2)	172(3)	Host–guest
H·DMA					
O1A–H1A···O2A	0.84	1.82	2.655(2)	171.1	Intramolecular
O2A–H3A···O6	0.84	1.81	2.604(16)	157.3	Host–guest
O2A–H3A···O5	0.84	1.93	2.75(3)	165.7	Host–guest
O1B–H1B···O2B	0.84	1.86	2.687(2)	168.7	Intramolecular
O2B–H3B···O7	0.84	1.95	2.77(2)	166.3	Host–guest
O2B–H3B···O8	0.84	1.77	2.571(13)	159.2	Host–guest

[a] Symmetry operator: 1 + *x*, *y*, *z*.

Table 3 Torsion angles

		H·NMF	H·NMA	H·DMF	H·DMA
τ_1	Mol 1	−17.2(4)	−18.9(5)	−13.0(2)	−25.6(3)
	Mol 2	−21.7(3)	−21.1(4)	—	−22.5(3)
τ_2	Mol 1	−53.4(3)	−54.0(4)	−73.2(2)	−55.9(2)
	Mol 2	−47.3(3)	−65.5(4)	—	−63.0(2)
τ_3	Mol 1	−20.4(3)	−20.9(4)	−25.42(2)	−13.0(3)
	Mol 2	−16.7(3)	−16.5(4)	—	−14.2(3)
τ_4	Mol 1	−58.0(3)	−54.8(4)	−61.7(2)	−71.6(2)
	Mol 2	−57.8(3)	−65.7(4)	—	−72.0(2)
τ_5	Mol 1	−69.0(3)	−68.2(3)	−66.1(2)	−176.6(2)
	Mol 2	−67.9(2)	−69.2(4)	—	−176.0(2)
τ_6	Mol 1	−98.5(3)	−98.0(3)	−95.3(2)	−97.4(2)
	Mol 2	−97.7(2)	−95.4(4)	—	−99.1(2)

the cell. These are shown in Fig. 1, in which the host molecules display a similar conformation which is governed by an intramolecular O–H···O hydrogen bond, while the second hydroxyl moiety acts as a hydrogen bond donor to the guest NMF. A further aspect of the host conformation is that of the four torsion angles of the phenyl rings (τ_1–τ_4), the torsion angle which describes the twist of the cyclohexyl moiety (τ_5), and the torsion angle subtended by the two chiral carbon atoms of the five membered ring (τ_6). The metrics of the hydrogen bonds and the values of the torsion angles for all the structures are given in Tables 2 and 3, respectively. The packing of the H·NMF structure is shown in Fig. 1. Each NMF molecule is H-bonded to a host *via* (host)O–H···O=(guest) interactions. The structure is characterised by continuous chains of hydrogen bonded NMF molecules in channels running in the direction [100]. The hydrogen bond pattern may be described in graph set notation as $C_2^2(8)$.[13] One of the NMF molecules is disordered over two positions with the site occupancies of 0.62/0.38. Inspection of the non-bonding interactions of these guests was carried out with the program Crystal Explorer[14] and the related fingerprint plots are shown separately in Fig. 2a–c. The spike labelled 1 is associated with the O=C(guest$_1$) accepting a hydrogen from (host)O–H and (guest$_2$)N–H. Spike 2 represents the donation of a hydrogen of (guest$_1$)N–H and (guest$_1$)–CH_3 to O=C(guest$_2$) acceptor. These features are repeated in Figs. 2b and c. The peak labelled 3 represents the H···H distances, which is a broad peak in Fig. 2a, while this area is more defined in Fig. 2b and c due to short distances between (guest$_2$)–CH_3 moiety and H atoms of neighbouring phenyl rings. We noted spike 4 on the fingerprint plots of the ordered and the minor component of the disordered guest which related to the (guest)–(CO)H interaction to the aromatic system of the phenyl ring of the host.

The structure of H·NMA is similar to that of H·NMF, but there are hydrogen bonded ribbons in which the hydrogen bonds

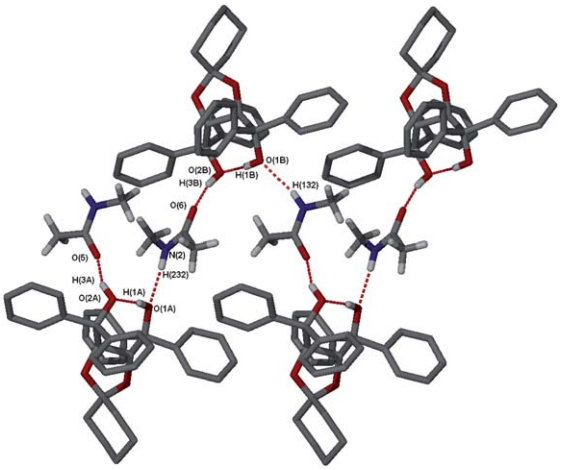

Fig. 3 Structure of H·NMA with $C_o^o(16)$ hydrogen bonded ribbons.

link alternate host$_1$···guest$_1$···host$_2$···guest$_2$ molecules, and can be described as $C_o^o(16)$. These run in channels in the direction [100] and are shown in Fig. 3.

The structure of H·DMF crystallises in the space group $P2_12_12_1$ with $Z = 4$. There are similarities with the previous structure in that we again have an intramolecular O–H···O hydrogen bond and a (host)O–H···O═(guest) with the O···O distance of 2.65 Å, however, the DMF molecules are trapped in cages formed by the surrounding host molecules (Fig. 4).

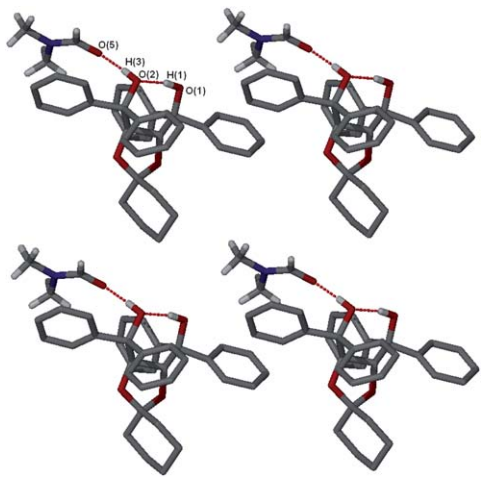

Fig. 4 Entrapped DMF molecules in H·DMF structure.

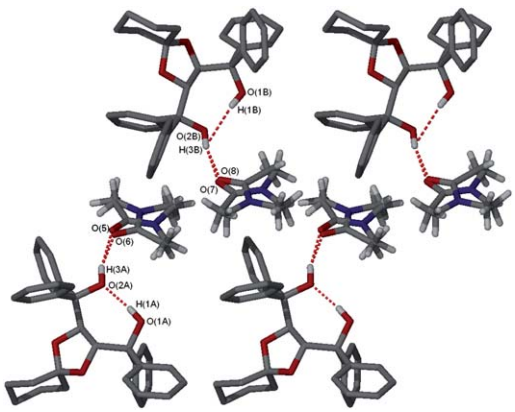

Fig. 5 The structure of H·DMA shows disorder in the guest positions.

The H·DMA structure crystallises in $P1$ with $Z = 2$ and shows disorder in the DMA molecules, as represented in Fig. 5. The site occupancies of the DMA refined to 0.66/0.34 and 0.63/0.37. Again we note (host)O–H···O═(guest) discrete H-bonds with O···O distance ≈ 2.67 Å.

Selectivity

Competition experiments were set up to determine the selectivity of the host compound towards the series of guests from which it crystallised. For the two-component competition, the mixtures of two guests were prepared in vials in which the mole fraction of the two guests varied from 0 to 1 in steps of 0.1. A fixed amount of host was added and dissolved by gentle heating and stirring. The ratio of total guest to host was never less than 20 : 1, to ensure that there was sufficient guest of lower mole fraction for efficient competition. The resultant crystals were removed from the mother liquor, dried over filter paper and analysed by ^{1}H NMR spectroscopy.

The results of two competition experiments are shown in Fig. 6 in which the mole fraction of a given guest in solution (X), on the abscissa, is plotted against its mole fraction in the solid state (Z) on the ordinate. Fig. 6a shows that DMF is preferentially enclathrated over NMF virtually over the complete composition mixture and reaches complete DMF selectivity with $X_{DMF} \geq 0.7$. Fig. 6b shows that the DMF–DMA

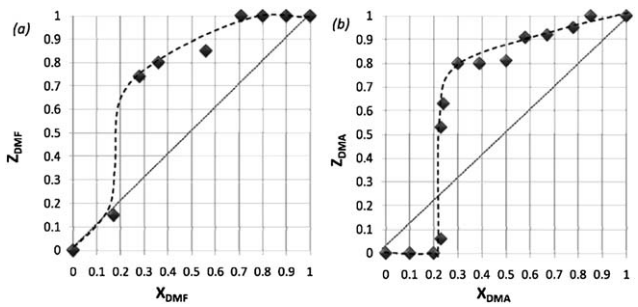

Fig. 6 Results of competition experiments between (a) DMF–NMF and (b) DMA–DMF.

Table 4 Selectivity constants

B \ A	NMF	DMF	NMA	DMA
NMF		4.71	1.13	9.00
DMF			0.09	4.47
NMA				8.1
DMA				

selectivity curve is sigmoidal and DMA is only preferred over DMF when $X_{DMA} > 0.22$.

Paucity of this material prevented us from carrying out complete selectivity curves for the remaining four guest pairs, and so we restricted our competition experiments to equimolar mixtures of the guests. The results of the selectivity constants for the six pairs, given as $K_{A:B} = Z_A/Z_B \times X_B/X_A$ with $X_A = X_B = 0.5$, are shown in Table 4. We observed the following large selectivity constants: $K_{DMA:NMF} = 9.0$, $K_{DMA:NMA} = 8.1$ and $K_{DMF:NMA} = 11.1$ ($K_{NMA:DMF} = 0.09$). There is virtually no discrimination between NMF and NMA with $K_{NMA:NMF} = 1.1$, so that the overall competition experiments show that this host discriminates as follows:

$$NMF \approx NMA < DMF < DMA$$

We noted above that the conformation of the host is governed by the intramolecular hydrogen bond (O–H···O) and the six torsion angles τ_1–τ_6. The intramolecular hydrogen bond is virtually constant with $d_{O\cdots O}$ ranging from 2.65 to 2.73 Å (Table 2). This locks the two hydroxyldiphenyl moieties in a practically fixed conformation, with τ_6 varying from −95.3 to −99.0°. The intermolecular hydrogen bond, linking the host hydroxyl hydrogen to the oxygen of the guest carbonyl moiety, is also invariant with O···O distances varying from 2.57 to 2.77 Å. We reasoned therefore that the mechanism for guest selectivity is dependent on the torsion angles which govern the conformation of the four phenyl rings (Table 3). We have plotted these placing the guests in the sequence obtained in the selectivity experiments, namely NMF, NMA, DMF and DMA (Fig. 7). We note that the four structures fall into two groups: H·NMF–H·NMA and H·DMF–H·DMA. The two former structures are isostructural with respect to the host positions, with the NMF/NMA guests

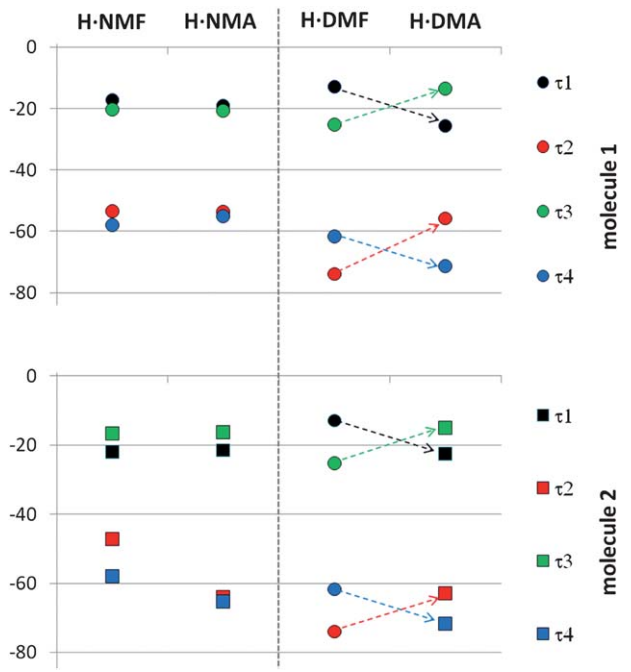

Fig. 7 Graphical summary of torsion angles.

Table 5 Packing factors (PFs)[a]

		H·NMF	H·NMA	H·DMF	H·DMA
V_{mol}/Å^3	Mol 1	58.0	74.1	74.6	91.9
	Mol 2	57.8	74.0	—	92.3
V_{void}/Å^3	Mol 1	147.3	174.5	129.8	150.9
	Mol 2	119.2	167.7	—	158.8
V_{mol}/V_{void} = PF%	Mol 1	39.4	42.5	57.5	60.9
	Mol 2	48.4	44.1	—	58.1
Average PF%		**43.9**	**≈ 43.3**	**< 57.5**	**< 59.5**

[a] V_{mol}—molecular volume and V_{void}—void volume. When a guest molecule was disordered, we report the average of the two disordered entities.

located in channels and all torsion angles (τ_1–τ_6) are essentially similar. In contrast, the torsion angles for H·DMF and H·DMA all cross over and effectively exchange values. Analysis of the packing of these structures reveals that the DMF molecule is associated with phenyl ring$_4$ and is parallel to it, with its non-hydrogen atoms averaging 3.2 Å from the mean plane of the ring. The same feature occurs with the H·DMA structure, but this time the disordered DMA guest lies parallel but further from ring$_2$ with its non-hydrogen atoms averaging 3.5 Å from the plane. In addition the DMA structure has a flipped cyclohexyl moiety with $\tau_5 \approx 176°$, and the host packing is such that these cyclohexyl rings are away from the DMA guest, their conformational changes do not effect directly the guest cavity (Fig. 5).

It is interesting to note that the space available for the guests correlates with the selectivity of the host. We have calculated the volumes of the guest molecules (V_{mol}) and their available space (V_{void}) by using the program MSRoll,[15] and their ratio, which represents the packing factor (PF%). Data for the packing factor calculation are given in Table 5. The void space pertaining to the H·NMF structure, molecule 2, yielded an unexpectedly low value of 119.2 Å^3, significantly different from that attributed to molecule 1, which is 147.3 Å^3. This occurrence related to the extended hydrogen bond network in the H·NMF structure which was discussed and shown in Fig. 2. We observe that the values of the packing factors vary in the order of NMF ≈ NMA < DMF < DMA which correlate to our results from the selectivity experiments. We noted a similar correlation between enantiomeric selectivity and guest available volume in the series of structures obtained with the same host and 2-butylamines of varying enantiomeric composition.[16]

Conclusions

In all four structures, the main host : guest hydrogen bond is of the type (host)–OH···O=C(guest) and its metrics are similar, with O···O distances varying in a narrow range. However, the secondary interactions between the guests and the various phenyl rings of the host are different. These give rise to inter-host spaces of different topologies and volumes, and analysis of the packing factor for the guests shows that the selectivity correlates with the available volume, so that, when the space is small, the corresponding guest is preferentially selected. It is gratifying that the competition experiments and the selectivity constants measured

by NMR are in agreement with the guest packing factors which were calculated from the structures.

References

1 M. R. Caira, L. R. Nassimbeni, D. Vujovic and E. Weber, *J. Chem. Soc., Perkin Trans. 2*, 2001, 861–863.
2 T. le Roex, L. R. Nassimbeni and E. Weber, *New J. Chem.*, 2008, **32**, 856–863.
3 G. R. Desiraju, *Crystal Engineering*, Elsevier, Amsterdam, 1989.
4 L. R. Nassimbeni, Perspectives in Supramolecular Chemistry, in *Separation and Reactions in Organic Supramolecular Chemistry*, ed. F. Toda and R. Bishop, John Wiley & Sons, Ltd, Chichester, 2004, vol. 8, ch. 5.
5 A. M. Pivovar, K. T. Holman and M. D. Ward, *Chem. Mater.*, 2001, **13**, 3018.
6 F. Toda, Molecular Inclusion and Molecular Recognition—Clathrates II, in *Topics in Current Chemistry*, Springer-Verlag, Berlin, 1988, vol. 149, pp. 211–238.
7 Bruker, *APEX2, Version 1.0-27*, Bruker AXS Inc, Madison, Wisconsin, USA, 2005.
8 Bruker, *SAINT-Plus (including XPREP), Version 7.12*, Bruker AXS Inc, Madison, Wisconsin, USA, 2004.
9 Bruker, *XPREP, Version 6.14*, Bruker AXS Inc, Madison, Wisconsin, USA, 2003.
10 G. M. Sheldrick, *SHELXS-97 and SHELXL-97 Programs for Crystal Structure Determination and Refinement*, University of Göttingen, 1997.
11 L. J. Barbour, *J. Supramol. Chem.*, 2001, **1**, 189–191.
12 A. L. Spek, *PLATON, A Multipurpose Crystallographic Tool*, Utrecht University, Utrecht, The Netherlands, 2008.
13 S. Eppel and J. Bernstein, *Acta Crystallogr.*, 2008, **B64**, 50–56.
14 (*a*) J. J. McKinnon, M. A. Spackman and A. S. Mitchell, *Acta Crystallogr.*, 2004, **B60**, 627; (*b*) M. A. Spackman and J. J. McKinnon, *CrystEngComm*, 2002, **4**, 378.
15 M. L. Connolly, *J. Mol. Graphics*, 1993, 139–141.
16 N. B. Báthori and L. R. Nassimbeni, *Cryst. Growth Des.*, 2010, **10**(4), 1782–1787.